Tech Science Press

Teamwork Optimization with Deep Learning Based Fall Detection for IoT-Enabled Smart Healthcare System

Sarah B. Basahel[1], Saleh Bajaba[2], Mohammad Yamin[3], Sachi Nandan Mohanty[4] and E. Laxmi Lydia[5,*]

[1]Department of Management Information Systems, Faculty of Economics and Administration, King Abdulaziz University, Jeddah, Saudi Arabia
[2]Department of business Administration, Faculty of Economics and Administration, King Abdulaziz University, Jeddah, 21589, Saudi Arabia
[3]Department of Management Information Systems, Faculty of Economics and Administration, King Abdulaziz University, Jeddah, 21589, Saudi Arabia
[4]School of Computer Science &Engineering (SCOPE), VIT-AP University, Amaravati, Andhra Pradesh, India
[5]Department of Computer Science and Engineering, GMR Institute of Technology, Andhra Pradesh, Rajam 532127, India
*Corresponding Author: E. Laxmi Lydia. Email: elaxmi2002@yahoo.com
Received: 30 September 2022; Accepted: 19 November 2022

Abstract: The current advancement in cloud computing, Artificial Intelligence (AI), and the Internet of Things (IoT) transformed the traditional healthcare system into smart healthcare. Healthcare services could be enhanced by incorporating key techniques like AI and IoT. The convergence of AI and IoT provides distinct opportunities in the medical field. Fall is regarded as a primary cause of death or post-traumatic complication for the ageing population. Therefore, earlier detection of older person falls in smart homes is required to improve the survival rate of an individual or provide the necessary support. Lately, the emergence of IoT, AI, smartphones, wearables, and so on making it possible to design fall detection (FD) systems for smart home care. This article introduces a new Teamwork Optimization with Deep Learning based Fall Detection for IoT Enabled Smart Healthcare Systems (TWODL-FDSHS). The TWODL-FDSHS technique's goal is to detect fall events for a smart healthcare system. Initially, the presented TWODL-FDSHS technique exploits IoT devices for the data collection process. Next, the TWODL-FDSHS technique applies the TWO with Capsule Network (CapsNet) model for feature extraction. At last, a deep random vector functional link network (DRVFLN) with an Adam optimizer is exploited for fall event detection. A wide range of simulations took place to exhibit the enhanced performance of the presented TWODL-FDSHS technique. The experimental outcomes stated the enhancements of the TWODL-FDSHS method over other models with increased accuracy of 98.30% on the URFD dataset.

Keywords: Internet of things; smart healthcare; deep learning; team work optimizer; capsnet; fall detection

1 Introduction

The Healthcare sector recently began to use information technology for formulating contemporary applications and improving the treatment and diagnostic process [1]. Advanced medical services will have numerous stakeholders: research and clinical centres, surgeons, and patients. Multiple dimensions concern clinical management, disease prevention initiatives and observation, treatment and prognosis, medical studies, health, and decision-making [2]. For example, Artificial Intelligence (AI), mobile internet, big data, microelectronics, 5G systems, and Cloud Computing (CC), together with smart biotechnology, were considered indicators of the latest health care. Such techniques will be used in each stage of advanced healthcare [3]. From patients' viewpoint, portable or wearable gadgets are enforced to monitor their health as required. From the perceptive of doctors, a smart clinical decision-supporting mechanism is enforced to guide and enhance the diagnostic process [4].

The data, captured through incorporated, portable, and ingestible sensors, mobile paradigms, and device-used paradigms, allow the author to know users' habits [5]. With additional data sets, it becomes possible to expose their medical condition by applying Deep Learning (DL) or Machine Learning (ML) related techniques. Conventional cloud technologies that depend on methods for big data analysis were enforced to render scalability, optimum performances, and support non-safety along with the delay-related IoT fields [6]. But suppose the patient is serious about the readiness of inadequate sources and whenever they need a high mark of accessibility and efficiency. In that case, the interruption from the core network or latency variance may intensely generate adverse effects and lead to dreadful significance during emergencies.

Falling will is a common issue faced by older adults. For elder ones, a fall is highly risky and may cause severe health problems [7]. In addition, falls and lack of balance is life-threatening disease symptoms. Often, the person cannot rise without support and needs immediate medical deliberation. Fear of falling surges negative post-fall impacts and might reduce patient confidence. Therefore, it would limit patients' activities, diminish social communication, and ultimately result in depression [8]. Then it helps to lessen medication costs and increase the opportunity for recovery. Authors have classified fall detection mechanisms into three classes ambience sensors, cameras, and wearable devices [9]. The system depends upon wearable devices is common since it can find a fall accurately nevertheless of patient location (i.e., indoor and outdoor) and does not disturb the privacy of persons and everyday activities [10]. Due to their asset restrictions (for instance, limited power and storage capacity), it should have a new technique that helps to decline heavy computation loads on wearable nodes while enhancing or preserving the QoS.

This article introduces a new Teamwork Optimization with DL-based Fall Detection for IoT Enabled Smart Healthcare Systems (TWODL-FDSHS). The TWODL-FDSHS technique's goal is to detect fall events for a smart healthcare system. Initially, the presented TWODL-FDSHS technique exploits IoT devices for the data collection process. Next, the TWODL-FDSHS technique applies the TWO with Capsule Network (CapsNet) model for feature extraction. At last, a deep random vector functional link network (DRVFLN) with Adam optimizer was exploited for fall event detection. A wide range of simulations was conducted to exhibit the enhanced performance of the presented TWODL-FDSHS technique.

2 Literature Review

Qian et al. [11] introduce a wearable fall detection (FD) mechanism that depends on a new multi-level threshold approach. This technique will combine Micro-Electro-Mechanical-Systems (MEMS) with that narrowband IoT. This mechanism even adds user interfaces for healthcare specialists based

on the server-client architecture and cloud technology. Salah et al. [12] mainly focus on displaying the efficiency of FD in a resource-limited microcontroller at the network edge by using wearable accelerometers. As the hardware sources of microcontrollers were limited, a lightweight FD in the DL method has been advanced for deploying over microcontrollers with some kilobytes of memory. The microcontroller has been deployed in a low-power wide area network depending on long-range (LoRa) transmission technology. Lin et al. [13] devise a new FD method related to an LSTM framework and a set of commercial lightweight smart insoles with a trained referencing denoising AE (RDAE). Through the comparison made with conventional AEs, the referencing sub-path RDAE can be included to attain the automatic extraction of features.

Vaiyapuri et al. [14] modelled an IoT-assisted elderly FD method utilizing optimum deep CNN (IMEFD-ODCNN) for smart home care. This IMEFD-ODCNN focused on enabling smartphones and intellectual DL techniques for detecting fall occurrence in the smart home. Also, the SqueezeNet method was used as a feature-extracting method for deriving suitable feature vectors for FD. Moreover, the parameter tuning of the SqueezeNet method is carried out through the salp swarm optimized (SSO) method. Lastly, the sparrow search optimization algorithm (SSOA), including VAE, named SSOA-VAE related technique, was used to classify non-fall and fall events. Chuma et al. [15] propose a smart FD mechanism related to IoT for monitoring the older person with your privacy-protected. Now, FD has allured important research attention, and DL has witnessed a good presentation in this task by means of orthodox cameras. This study devises a new FD system that would use a continual-wave Doppler radar sensor for procuring the elderly movements and transfer this data through the internet to a server by DL utilizing a CNN that finds the fall.

In [16], a HOG-SVM-related FD in IoT mechanism for older people was modelled. To assure privacy and be robust to variations of light intensity, deep sensors are used in place of RGB cameras to receive the binary images of aged people. After procurement of the denoised binary images, the characteristics of individuals were derived through a histogram of the oriented gradient. Image classification can be effected to determine fall status with the help of the linear SVM. In [17], the authors address this issue by presenting an FD System related to IoT (FallDS-IoT) by framing wearable systems for FD of older adults. The authors utilize Gyroscope sensors and an Accelerometer to get precise outcomes of FD. The authors classified the daily actions of older persons into falling, sleeping, walking, and sitting. The authors leverage 2 renowned ML approaches, such as a decision tree and a K-NN algorithm, to manage the above work.

3 The Proposed Method

In this article, a new TWODL-FDSHS approach was devised for smart healthcare. The major intention of the presented TWODL-FDSHS technique lies in detecting fall events for a smart healthcare system. Primarily, the presented TWODL-FDSHS technique exploited the IoT devices for the data collection. Then, the TWODL-FDSHS technique encompasses CapsNet feature extraction, TWO-based hyperparameter tuning, DRVFLN-based fall detection, and Adam optimizer. Fig. 1 depicts the workflow of the TWODL-FDSHS system.

3.1 Feature Extraction

The TWODL-FDSHS technique applies TWO with the CapsNet model for feature extraction in this work. Capsule networks can encode spatial information and discriminate between different poses, textures, and orientations [18]. A capsule refers to a collection of neurons. Every capsule has an activity vector related to them, which capture many instantiation parameters for detecting specific kind of

objects or its part. The orientation and length of the present vector probability or the likelihood of its generalized pose and existence of that object. This vector is passed onto the upper-level capsule from the lower-layer capsule. A coupling coefficient exists between the capsule layers. When the output of the existing capsule is matched with the lower level capsule matches, then the coupling coefficient rises, calculated using the *softmax* function. Specifically, once the existing capsule identifies a tight cluster of preceding predictions and indicates the incidence of that object, it leads to a higher probability, called routing by agreement.
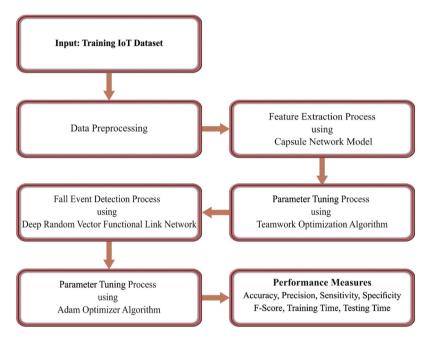

Figure 1: Working process of proposed model

Initially, the predictive vector is calculated by,

$$\hat{u}_{j|i}\wedge = W_{ij}u_i, \tag{1}$$

In Eq. (1), $\hat{u}_{j|i}$ represent the prediction or output vector of the upper-level *j-th* capsules, W_{ij} and u_i denote the weighted matrices and predictive vector of *i-th* capsules in the lower layer correspondingly. It captures spatial relations and relationships between objects and sub-objects.

$$c_{ij} = exp(b_{ij}) \bigg/ \sum exp\,(b_{ik}) \tag{2}$$

The coupling coefficient is calculated using the *softmax* function based on the degree of agreement between adjoining layer capsules.

where b_{ij} indicates log probability among the 2 capsules, initialized to zero, and k signifies capsule count. The input vector s_j to the *j-th* layer capsules that weighted sum of $\hat{u}_{j|i}\wedge$ vector studied using the routing method is evaluated by,

$$s_j = \sum_i c_{ij}\hat{u}_{j|i} \tag{3}$$

At last, a squashing function will combine squashing, and unit scaling is employed for confining output values within [0,1] as,

$$v_j = \frac{\|s_j\|^2}{1 + \|s_j\|^2} \frac{s_j}{\|s_j\|} \tag{4}$$

The loss function is related to the capsule in the final layer, whereas $m+$ $aưd$ $m-$ was fixed to 0.9 and 0.1 resp.

$$l_k = T_k \max(0, m^+ - ||v_k||)^2 + \lambda(1 - T_k) \max(0, ||v_k|| - m^-)^2 \tag{5}$$

where value T_k was 1 for a correct label or else, λ represents constant values set to 0.5.

3.2 Hyperparameter Tuning

For the hyperparameter tuning procedure, TWO algorithms are used. The main idea is to design a TWO algorithm comprised of reactions, activities, and behaviours amongst the team members to accomplish the team's major objective [19].

Solitary Activity: Every team member, based on personal efforts and behaviours, strives to contribute to the achievement of the whole group. In a mathematical model, every member of the population is determined by the vector, and the number of problem parameters is precisely similar to the component count. From the expression, the algorithm population makes use of the matrixes where the column count is equivalent to the number of variables, along with the row count is being similar to the population member.

$$X = \begin{bmatrix} X_1 & X_{1,1} & \dots & X_{1,d} & \dots & X_{1,n} \\ \vdots & \vdots & \ddots & \vdots & & \vdots \\ X_i & X_{i,1} & \dots & X_{i,d} & \dots & X_{i,n} \\ \vdots & \vdots & & \vdots & \ddots & \vdots \\ X_M & X_{M,1} & \dots & X_{M,d} & \dots & X_{M,n} \end{bmatrix}_{M \times n} \tag{6}$$

From the expression, M illustrates the member count in the group, X indicates the individual matrixes of the teamwork optimization approach, $x_{i,d}$ indicates the d-th parameter specified as the team member i-th, and n indicates the number of problem parameters. The following equation defines the value of the fitness function (FF).

$$F = \begin{bmatrix} F_1 & F(X_1) \\ \vdots & \vdots \\ F_i & F(X_i) \\ \vdots & \vdots \\ F_M & F(X_M) \end{bmatrix} \tag{7}$$

F indicates the FF from the equation, and F_i determines the FF value for i-th group numbers. Based on the target function, the supervisor is an individual that implements better amongst the individual groups. The supervisor's task is to lead the group member to accomplish the major objective.

Supervisor: $S = X_s$ and s indicate the team member row number with the minimum value of the F vector. Where S indicates the team supervisor.

Phase1: leadership of a supervisor

In these phases, the group individual has been rehabilitated based on the supervisor's guidelines. Meanwhile, the supervisor reported their data to be the residual group individual and led the individual towards the team. The following equation has demonstrated these steps of the upgrade in the presented technique.

$$X_i^{S1}: x_{i,d}^{S1} = x_{i,d} + a \times (S_d - K \times x_{i,d}) \tag{8}$$

$$X_i = \begin{cases} X_i^{S1}, & F_i^{S1} < F_i \\ X_i, & else \end{cases} \tag{9}$$

$$K = round\,(1 + a) \tag{10}$$

Now, X_i^{S1} indicates the new location for the *i-th* team members based on the supervisor's guidelines and leadership. F_i^{S1} represent the FF value, $\chi_{i,d}^{S1}$ denotes the new quantity for the *d-th* variable developed by means of *i-th* group individuals rehabilitated based on the supervisor guidance, *a* demonstrates an arbitrarily chosen number within [0,1], and *K* illustrates the update-index.

Phase2: Sharing information

For increased team performance, every team member is struggling to employ the other team member data that works better than others and it is formulated in the subsequent equation.

$$lx^{N,i}: x_d^{N,i} = \frac{\sum_{j=1}^{M_i} \chi_{j,d}^{g,i}}{M_i} \tag{11}$$

$$X_i^{S2}: x_{i,d}^{S2} = x_{i,d} + a \times (x_d^{N,i} - K \times x_{i,d}) \times sign\,(F_i - F^{N,i}) \tag{12}$$

$$X_i = \begin{cases} X_i^{S2}, & F_i^{S2} < F_i \\ X_i, & else \end{cases} \tag{13}$$

Now, $X^{N,i}$ indicates the team member average that is enhanced than *i-th*, $F^{N,i}$ illustrates the FF value, M_i determines the number of team members which implements properly towards the *i-th* group individuals, $\chi_{j,d}^{g,i}$ defines the *d-th* variables recommended number using the *j-th* members of the team that implements effectively when compared to *i-th* team members, X_i^{S2} demonstrates the novel location of *i-th* team members and F_i^{S2} illustrates value of FF.

Phase 3: Solitary activity

Every member of the team strives to improve their own functioning based on the upgraded location:

$$X_i^{S3}: x_{i,d}^{S3} = \chi_{i,d} + (-0.01 + a \times 0.02) \times \chi_{i,d} \tag{14}$$

$$X_i = \begin{cases} X_i^{S3}, & F_i^{S3} < F_i \\ X_i, & else \end{cases} \tag{15}$$

Now, X_i^{S3} illustrates the location of *i-th* team members and F_i^{S3} indicates the value of FF.

The TWO approaches derived a FF to accomplish better classifier performance. It sets a positive value to characterize the good performance of the candidate solution. The reduction of the classifier error rate was regarded as a FF as follows.

$$fitness\,(x_i) = ClassifierErrorRate\,(x_i) = \frac{no.\ of\ misclassified\ instances}{Total\ number\ of\ instances} * 100 \tag{16}$$

3.3 Fall Detection Using Optimal DRVFLN Model

Finally, the DRVFLN model with Adam optimizer is exploited for fall event detection. The presented method is an expanded edition of shallow RVFL networks from the context of DL or representation learning [20]. The DRVFLN network is regarded as a stacked hierarchy of hidden layers. Fig. 2 illustrates the infrastructure of RVFL. While the stacked hierarchical organization of hidden layers from the DRVFLN network allows common flexibility from size (of network depth and width) as follows:

$$H^{(1)} = g\left(XW^{(1)}\right) \tag{17}$$

$l > 1$ is defined by:

$$H^{(l)} = g\left(H^{(l-1)}W^{(l)}\right) \tag{18}$$

In Eq. (18), $W^{(1)} \in \mathbb{R}^{d \times N}$ and $W^{(l)} \in \mathbb{R}^{N \times N}$ correspondingly indicate the weighted matrix among the input-1st hidden layer and inter-hidden layers. This parameter (weight and bias) of hidden neurons was randomly generated from a suitable range. g indicates the non-linear activation function as follows:

$$D = \left[H^{(1)}H^{(2)} \dots H^{(L-1)}H^{(L)}X\right] \tag{19}$$

This design approach is like the shallow RVFL network where input-output layers have non-linear features under stacked hidden layers and novel features:
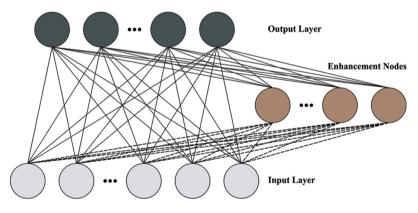
$$Y = D\beta_d \tag{20}$$

Figure 2: Structure of RVFL

The resulting weight $\beta_d \in \mathbb{R}^{(NL+d) \times K}$ (K: the class count) is resolved. DRVFLN to be a linear group among the feature and resulting layer weighted matrices β_d, the weighted sum of features under the hidden layer comprising the input layer. The training stage directly permits the technique for weight differently participation of each kind of feature originating in more than one layer.

Note that the proposed method splits themselves under the deep ESN under the following characteristics: the significant difference between deeper ESN and DRVFLN goes to the class of randomized RNN, but DRVFLN should randomize the feedforward technique. Hence, it has dissimilar target problems. It inspected the effectiveness of DRVFLN from classifier issue however deep ESN discovered a time-series issue. Moreover, DRVFLN is based on a shallow RVFL network with a resulting layer

encompassing nonlinearly changed features and novel features using a direct connection. Conversely, deep ESN doesn't consider original features under resulting weight computation.

At last, the DL structure, DRVFLN was generic and is employed by few RVFL variances. The Adam optimizer is utilized for the optimum selection of the hyperparameter of the DRVFLN method [21]. It is a widely applied step size method in the NN fields. The steps included in the Adam optimizer are shown in Algorithm 1. Early study denotes that the Adam optimizer can able to show a higher convergence rate than others.

Algorithm 1: Pseudocode of Adam Optimizer

Data: $\eta_t := \dfrac{\eta}{\sqrt{t}}$-step size, $\beta_1, \beta_2 \in (0, 1)$-decay rate for moment estimation, $\beta_{1,t} := \beta_1 \lambda^{t-1}$ with $\lambda \in (0, 1), \varepsilon > 0, e(w(t))$ as a convex distinguishable error function and $w(0)$ as initialized weight vectors

Determine $m_0 = 0$
Determine $v_0 = 0$
Determine $t = 0$
while $w(t)$ unconverged do
$t = t + 1$
$g_t = \nabla_w e(w(t-1))$
$m_t = \beta_{1,t} m_{t-1} + (1 - \beta_{1,t}) g_t$
$v_t = \beta_2 v_{t-1} + (1 - \beta_2) g_t^2$
$\hat{m}_t = \dfrac{m_t}{(1 - \beta_1^t)}$
$\hat{v}_t = \dfrac{v_t}{(1 - \beta_2^t)}$
$w(t) = w(t-1) - \eta_t \dfrac{\hat{m}_t}{(\sqrt{\hat{v}_t} + \varepsilon)}$
end
display $w(t)$

---

4 Result and Discussion

This section examines the performance of the TWODL-FDSHS method on MCF [22] and UR fall detection [23] datasets. Some sample fall detection images are demonstrated in Fig. 3. The parameter settings are given as follows: learning rate: 0.01, dropout: 0.5, batch size: 5, epoch count: 50, and activation: ReLU.

Table 1 provides brief fall detection results of the TWODL-FDSHS model on the MCF dataset. The results inferred that the TWODL-FDSHS model had shown enhanced fall detection outcomes under all sample sizes. It is noted that the TWODL-FDSHS model has reached an average $accu_y$ of 99.79%, $prec_n$ of 99.78%, $sens_y$ of 99.87%, $spec_y$ of 99.63%, and F_{score} of 99.72%.

Figure 3: Sample images

Table 1: Fall detection analysis of TWODL-FDSHS algorithm with various measures under the MCF dataset

Sample size (%)	Accuracy	Precision	Sensitivity	Specificity	F-score
80:20	99.87	99.54	99.82	99.60	99.87
70:30	99.78	100.00	99.88	99.70	99.97
60:40	99.76	99.82	99.87	99.86	99.32
50:50	99.74	99.86	99.90	99.55	99.88
40:60	99.82	99.70	99.88	99.45	99.54
Average	99.79	99.78	99.87	99.63	99.72

The training accuracy (TRA) and validation accuracy (VLA) obtained by the TWODL-FDSHS technique under the MCF database is depicted in Fig. 4. The experimental result denoted the TWODL-FDSHS method has attained maximal values of TRA and VLA. Seemingly the VLA is superior to TRA.

The training loss (TRL) and validation loss (VLL) attained by the TWODL-FDSHS method under the MCF dataset are displayed in Fig. 5. The experimental outcome indicated the TWODL-FDSHS method had exhibited the least values of TRL and VLL. Particularly, the VLL is lesser than TRL.
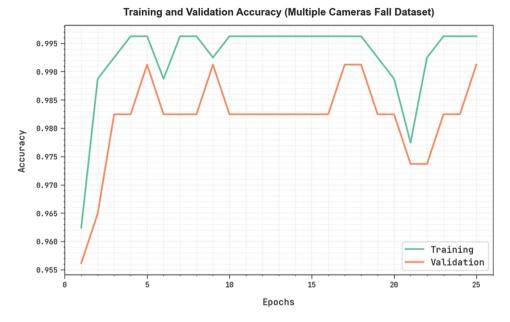
Training and Validation Accuracy (Multiple Cameras Fall Dataset)

Figure 4: TRA and VLA analysis of TWODL-FDSHS algorithm under MCF dataset

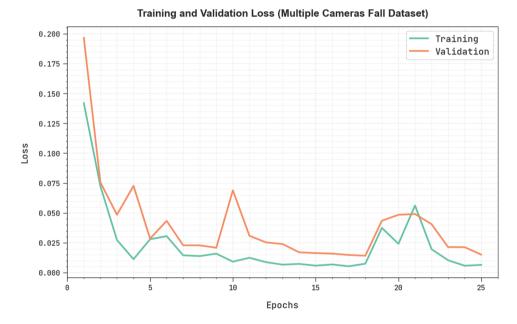**Training and Validation Loss (Multiple Cameras Fall Dataset)**

Figure 5: TRL and VLL analysis of TWODL-FDSHS algorithm under MCF dataset

Table 2 offers brief fall detection results of the TWODL-FDSHS technique on the URFD dataset. The results denoted the TWODL-FDSHS approach has exhibited enhanced fall detection outcomes under all sample sizes. It is noted that the TWODL-FDSHS method has reached an average $accu_y$ of 99.62%, $prec_n$ of 99.84%, $sens_y$ of 99.76%, $spec_y$ of 99.75%, and F_{score} of 99.71%.

Table 2: Fall detection analysis of TWODL-FDSHS algorithm with various measures under the URFD dataset

Sample size (%)	Accuracy	Precision	Sensitivity	Specificity	F-score
80:20	99.89	99.76	99.95	99.97	99.87
70:30	99.61	99.80	99.64	99.68	99.87
60:40	99.55	99.99	99.51	99.47	99.66
50:50	99.55	99.92	99.82	99.91	99.58
40:60	99.49	99.72	99.89	99.73	99.56
Average	99.62	99.84	99.76	99.75	99.71

The TRA and VLA gained by the TWODL-FDSHS method under the URFD dataset are shown in Fig. 6. The experimental outcome indicated the TWODL-FDSHS approach has attained maximal values of TRA and VLA. Seemingly the VLA is superior to TRA.
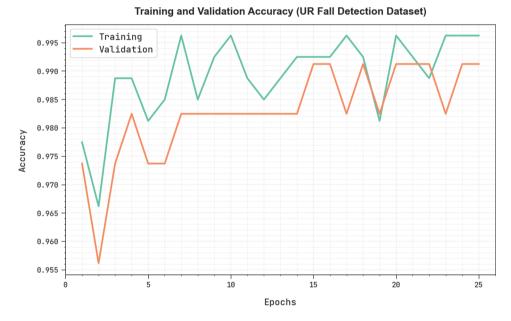

Figure 6: TRA and VLA analysis of TWODL-FDSHS algorithm under URFD dataset

The TRL and VLL obtained by the TWODL-FDSHS method under the URFD dataset are shown in Fig. 7. The experimental result represented the TWODL-FDSHS approach has exemplified the least values of TRL and VLL. Particularly, the VLL was lesser than TRL.

Table 3 and Fig. 8 report a comparison study of the TWODL-FDSHS model in terms of $accu_y$ on MCF dataset [24]. The results established the 1D-CNN and 2D-CNN methods have reported lower $accu_y$ values of 94.53% and 95.75% respectively. Next, the ResNet-50, ResNet-101, and depthwise methods have exhibited reasonable $accu_y$ of 96.11%, 96.65%, and 97.51% respectively. Although the IMEFD-ODCNN model has reached near optimal $accu_y$ of 99.71%, the TWODL-FDSHS model has outperformed the existing models with maximum $accu_y$ of 99.79%.

Figure 7: TRL and VLL analysis of TWODL-FDSHS algorithm under URFD dataset

Table 3: $Accu_y$ Analysis of TWODL-FDSHS algorithm with recent systems under MCF dataset

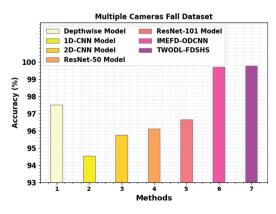| Methods	Accuracy (%)
Depthwise	97.51
1D-CNN	94.53
2D-CNN	95.75
ResNet-50	96.11
ResNet-101	96.65
IMEFD-ODCNN	99.71
TWODL-FDSHS	99.79

Figure 8: $Accu_y$ analysis of TWODL-FDSHS algorithm under MCF dataset

Table 4 and Fig. 9 report a comparative analysis of the TWODL-FDSHS approach in terms of $accu_y$ on the URFD dataset. The outcomes illustrated the 1D-CNN and 2D-CNN techniques have stated lower $accu_y$ values of 92.99% and 95.07% correspondingly. Next, the ResNet-50, ResNet-101, and depthwise methods have displayed reasonable $accu_y$ of 95.65%, 95.96%, and 98.30% correspondingly. Although the IMEFD-ODCNN approach has acquired reached near optimal $accu_y$ of 99.32%, the TWODL-FDSHS technique has exemplified the existing algorithms with a maximum $accu_y$ of 99.62%.

Table 4: $Accu_y$ analysis of TWODL-FDSHS algorithm with recent systems under URFD dataset

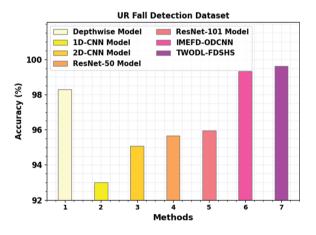| Methods	Accuracy (%)
Depthwise Model	98.30
1D-CNN Model	92.99
2D-CNN Model	95.07
ResNet-50 Model	95.65
ResNet-101 Model	95.96
IMEFD-ODCNN	99.32
TWODL-FDSHS	99.62

Figure 9: $Accu_y$ analysis of TWODL-FDSHS algorithm under URFD dataset

Table 5 and Fig. 10 illustrate a comparative training time (TRT) and testing time (TST) assessment of the TWODL-FDSHS model on the MCF dataset. With respect to TRT, the TWODL-FDSHS model has shown a reduced TRT of 20.50 ms, whereas the depthwise, 1D-CNN, 2D-CNN, ResNet-50, ResNet-101, and IMEFD-ODCNN models have attained increased TRT of 49.60, 34.26, 33.17, 20.74, 25.80, and 20.50 ms respectively. At the same time, with respect to TST, the TWODL-FDSHS technique has exhibited a reduced TST of 7.80 ms whereas the depthwise, 1D-CNN, 2D-CNN, ResNet-50, ResNet-101, and IMEFD-ODCNN algorithms have attained increased TST of 19.57, 13.78, 15.36, 17.69, 18.17, and 8.07 ms correspondingly.

Table 5: TRT and TST analysis of TWODL-FDSHS algorithm with recent systems under MCF dataset

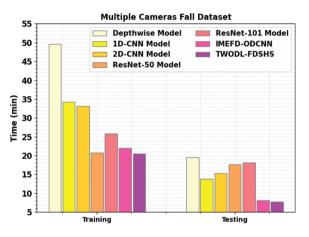| Methods	TRT (min)	TST (min)
Depthwise Model	49.60	19.57
1D-CNN Model	34.26	13.78
2D-CNN Model	33.17	15.36
ResNet-50 Model	20.74	17.69
ResNet-101 Model	25.80	18.17
IMEFD-ODCNN	21.98	8.07
TWODL-FDSHS	20.50	7.80

Figure 10: TRT and TST analysis of TWODL-FDSHS algorithm under URFD dataset

Table 6 and Fig. 11 exemplify a comparative TRT and TST assessment of the TWODL-FDSHS technique on URFD dataset. With respect to TRT, the TWODL-FDSHS technique has shown a reduced TRT of 13.24 ms, whereas the depthwise, 1D-CNN, 2D-CNN, ResNet-50, ResNet-101, and IMEFD-ODCNN algorithms have reached increased TRT of 21.10, 17.38, 20.95, 26.58, 26.83, and 13.52 ms, correspondingly. Simultaneously, with respect to TST, the TWODL-FDSHS approach has exhibited reduced TST of 9.52 ms whereas the depthwise, 1D-CNN, 2D-CNN, ResNet-50, ResNet-101, and IMEFD-ODCNN models have achieved increased TST of 10.22, 10.02, 9.82, 12.27, 18.05, and 13.17 ms correspondingly.

Table 6: TRT and TST analysis of TWODL-FDSHS algorithm with recent systems under URFD dataset

Methods	TRT (min)	TST (min)
Depthwise Model	21.10	10.22
1D-CNN Model	17.38	10.02

(Continued)

Table 6: Continued

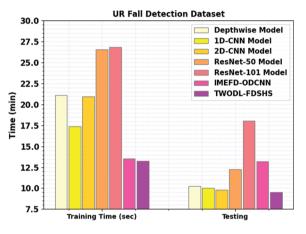| Methods	TRT (min)	TST (min)
2D-CNN Model	20.95	9.82
ResNet-50 Model	26.58	12.27
ResNet-101 Model	26.83	18.05
IMEFD-ODCNN	13.52	13.17
TWODL-FDSHS	13.24	9.52

Figure 11: TRT and TST analysis of TWODL-FDSHS algorithm under URFD dataset

These results ensured the enhanced performance of the TWODL-FDSHS model over other DL models.

5 Conclusion

In this article, a new TWODL-FDSHS algorithm was devised for smart healthcare. The major intention of the presented TWODL-FDSHS technique lies in the detection of fall events for a smart healthcare system. Primarily, the presented TWODL-FDSHS technique exploited the IoT devices for the data collection process. Followed by, the TWODL-FDSHS technique applied TWO with the CapsNet model for feature extraction. At last, the DRVFLN model with Adam optimizer is exploited for fall event detection. In order to exhibit the enhanced performance of the presented TWODL-FDSHS technique, a wide range of simulations were carried out. The experimental outcomes stated the enhancements of the TWODL-FDSHS algorithm over other models. In the future, the presented TWODL-FDSHS technique can be extended by utilizing advanced DL techniques for classifying purposes.

Conflicts of Interest: The authors declare that they have no conflicts of interest to report regarding the present study.

References

[1]   K. Rezaee, M. R. Khosravi and M. K. Moghimi, "Intelligent elderly people fall detection based on modified deep learning deep transfer learning and iot using thermal imaging-assisted pervasive surveillance," in *Intelligent Healthcare*, Singapore: Springer, pp. 113–132, 2022.

[2]   S. Neelakandan, J. R. Beulah, L. Prathiba, G. L. N. Murthy, E. F. Irudaya Raj *et al.,* "Blockchain with deep learning-enabled secure healthcare data transmission and diagnostic model," *International Journal of Modeling, Simulation, and Scientific Computing*, vol. 13, no. 4, pp. 2241006, 2022.

[3]   R. Tanwar, N. Nandal, M. Zamani and A. A. Manaf, "Pathway of trends and technologies in fall detection: A systematic review," *Healthcare*, vol. 10, no. 1, pp. 172, 2022.

[4]   M. E. Karar, H. I. Shehata and O. Reyad, "A survey of iot-based fall detection for aiding elderly care: Sensors, methods, challenges and future trends," *Applied Sciences*, vol. 12, no. 7, pp. 3276, 2022.

[5]   A. Ramachandran, A. Ramesh and A. Karuppiah, "Evaluation of feature engineering on wearable sensor-based fall detection," in *2020 Int. Conf. on Information Networking (ICOIN)*, Barcelona, Spain, pp. 110–114, 2020.

[6]   S. Yu, Y. Chai, H. Chen, R. A. Brown, S. J. Sherman *et al.,* "Fall Detection with wearable sensors: A hierarchical attention-based convolutional neural network approach," *Journal of Management Information Systems*, vol. 38, no. 4, pp. 1095–1121, 2021.

[7]   A. Tahir, W. Taylor, A. Taha, M. Usman, S. A. Shah *et al.,* "IoT based fall detection system for elderly healthcare," in *Internet of Things for Human-Centered Design, Studies in Computational Intelligence book series*, vol. 1011. Singapore: Springer, pp. 209–232, 2022.

[8]   G. Kyriakopoulos, S. Ntanos, T. Anagnostopoulos, N. Tsotsolas, I. Salmon *et al.,* "Internet of things (iot)-enabled elderly fall verification, exploiting temporal inference models in smart homes," *International Journal of Environmental Research and Public Health*, vol. 17, no. 2, pp. 408, 2020.

[9]   A. S. Pillai, S. Badgujar and S. Krishnamoorthy, "Wearable sensor and machine learning model-based fall detection system for safety of elders and movement disorders," in *Proc. of Academia-Industry Consortium for Data Science, Advances in Intelligent Systems and Computing Book Series*, Singapore, Springer, vol. 1411, pp. 47–60, 2022.

[10] P. Gharti, "A study of fall detection monitoring system for elderly people through IOT and mobile based application devices in indoor environment," in *2020 5th Int. Conf. on Innovative Technologies in Intelligent Systems and Industrial Applications (CITISIA)*, Sydney, Australia, pp. 1–9, 2020.

[11] Z. Qian, Y. Lin, W. Jing, Z. Ma, H. Liu *et al.,* "Development of a real time wearable fall detection system in the context of internet of things," *IEEE Internet of Things Journal*, vol. 9, no. 21, pp. 1, 2022. https://doi.org/10.1109/JIOT.2022.3181701.

[12] O. Z. Salah, S. K. Selvaperumal and R. Abdulla, "Accelerometer-based elderly fall detection system using edge artificial intelligence architecture," *International Journal of Electrical & Computer Engineering*, vol. 12, no. 4, pp. 4430, 2022.

[13] Z. Lin, Z. Wang, H. Dai and X. Xia, "Efficient fall detection in four directions based on smart insoles and RDAE-LSTM model," *Expert Systems with Applications*, vol. 205, no. 9, pp. 117661, 2022.

[14] T. Vaiyapuri, E. L. Lydia, M. Y. Sikkandar, V. G. Diaz, I. V. Pustokhina *et al.,* "Internet of things and deep learning enabled elderly fall detection model for smart homecare," *IEEE Access*, vol. 9, pp. 113879–113888, 2021.

[15] E. L. Chuma, L. L. B. Roger, G. G. de Oliveira, Y. Ianond and D. Pajuelo, "Internet of things (iot) privacy-protected, fall-detection system for the elderly using the radar sensors and deep learning," in *2020 IEEE Int. Smart Cities Conf. (ISC2)*, Piscataway, NJ, USA, pp. 1–4, 2020.

[16] X. Kong, Z. Meng, N. Nojiri, Y. Iwahori, L. Meng *et al.,* "A hog-svm based fall detection iot system for elderly persons using deep sensor," *Procedia Computer Science*, vol. 147, no. 1, pp. 276–282, 2019.

[17] S. K. Bhoi, S. K. Panda, B. Patra, B. Pradhan, P. Priyadarshinee *et al.,* "FallDS-IoT: A fall detection system for elderly healthcare based on iot data analytics," in *2018 Int. Conf. on Information Technology (ICIT)*, Bhubaneswar, India, pp. 155–160, 2018.

[18] C. Xiang, M. Su, C. Zhang, F. Wang, M. Yang *et al.,* "E-CapsGan: Generative adversarial network using capsule network as feature encoder," *Multimedia Tools and Applications*, vol. 81, no. 18, pp. 26425–26442, 2022.

[19] M. Dehghani and P. Trojovský, "Teamwork optimization algorithm: A new optimization approach for function minimization/maximization," *Sensors*, vol. 21, no. 13, pp. 4567, 2021.

[20] R. Sharma, T. Goel, M. Tanveer, S. Dwivedi and R. Murugan, "FAF-DRVFL: Fuzzy activation function based deep random vector functional links network for early diagnosis of Alzheimer disease," *Applied Soft Computing*, vol. 106, no. 3, pp. 107371, 2021.

[21] K. K. Kumar, "An efficient image classification of malaria parasite using convolutional neural network and adam optimizer," *Turkish Journal of Computer and Mathematics Education*, vol. 12, no. 2, pp. 3376–3384, 2021.

[22] E. Auvinet, C. Rougier, J. Meunier, A. St-Arnaud and J. Rousseau, "Multiple cameras fall dataset," DIRO-Université de Montréal, Montreal, QC, Canada, Tech. Rep. 1350, 2010.

[23] http://fenix.univ.rzeszow.pl/~mkepski/ds/uf.html.

[24] A. Sultana, K. Deb, P. K. Dhar and T. Koshiba, "Classification of indoor human fall events using deep learning," *Entropy*, vol. 23, no. 3, pp. 328, 2021.